JOURNAL OF SOLID STATE CHEMISTRY 6, 258–270 (1973)

Metal–Insulator Transition in V_nO_{2n-1}

SUKEJI KACHI, KOJI KOSUGE, AND HIDEYUKI OKINAKA

Department of Chemistry, Faculty of Science, Kyoto University, Kyoto, Japan

Received May 18, 1972

Research on phase relationships and structure studies by electron diffraction confirm V_nO_{2n-1} ($n = 3$–9) phases between V_2O_3 and VO_2. Metal–insulator phase transitions have been found in all phases but V_3O_5 and V_7O_{13}. Electrical, magnetic and thermodynamic properties associated with the transitions are reported for sintered samples or for single crystals prepared by a vapor-transport method. The results are collated and reviewed in summarized form.

Introduction

Hoschek and Klemm (*1*) first pointed out that there are a number of phases in the V–O system. Andersson (*2*) confirmed six intermediate phases of the form V_nO_{2n-1}($n = 3$–8) between V_2O_3 and VO_2. Later Andersson and Jahnberg (*3*) suggested that their structures might be triclinic, based upon the rutile structure with periodic "shear planes" resembling stacking faults in which extra planes of metal atoms are introduced.

Recently much interest has been focused upon the interesting structure of this homologous series. Since Wadsley (*4*) developed the concept of "crystallographic shear", the compounds that accommodate a deviation from ideal stoichiometry by planar defects have been a center of interest in solid state chemistry and physics. The present V_nO_{2n-1} series is one of the representatives that belong to the "shear-structure" compounds.

The electrical properties of some vanadium oxides, on the other hand, have attracted much attention of solid state scientists, since in 1959 Morin (*5*) publicized the metal–insulator transitions in V_2O_3 and VO_2 and reported (incorrectly) a similar transition in VO. Electrons in solids that interact weakly with neighboring-like atoms may be localized and hence best described by a Heitler–London model whereas those that interact strongly are well described by Bloch–Wilson band theory. Mott (*43*) has argued that there should be a sharp transition in the properties of the electrons on passing from the weak-interaction to the strong-interaction conditions. This idea present an interesting and challenging experimental problem to the physics and chemistry of solids. Vanadium oxides appear to exhibit both types of electrons. For this reason many investigations have been made on the magnetic, electrical and optical properties of these compounds. Extensive theoretical work has also been developed to account for the mechanism of the transition.

Recent reviews on the experiments and theories of this problem have been published by Adler (*6*), Mott and Zinamon (*7*), Goodenough (*8*), Hyland (*9*) and Suchet (*10*).

In this paper, the present authors aim to review and give new data of experimental results on the metal–insulator phase transitions in the V_nO_{2n-1} series, including physical and chemical properties that have been found in their laboratory over the past several years.

Phase Characterization (*11*)–(*14*)

For studies of this complex system, in particular in the initial stage of the research, thermodynamic characterization was of great importance. Figure 1 shows a schematic phase diagram of the V_2O_3–VO_2 system. The diagram was obtained by a quenching method: A number of specimens with various compositions prepared from the appropriate mixtures of V_2O_3 and V_2O_5 were heated in evacuated silica tubes for several days at various temperatures. The resulting phases were identified by X-ray and magnetic susceptibility measurements after quenching from reaction temperatures. Five intermediate phases, V_3O_5, V_4O_7,

Copyright © 1973 by Academic Press, Inc.
All rights of reproduction in any form reserved.

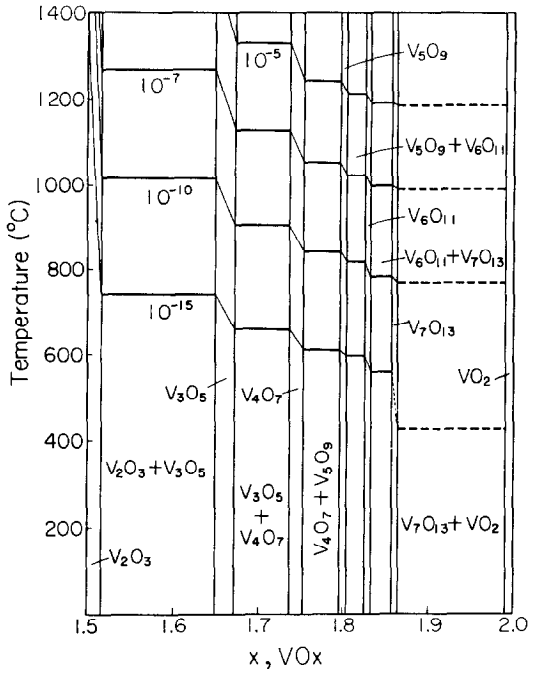

FIG. 1. Phase diagram of V_2O_3–VO_2 system with oxygen isobars.

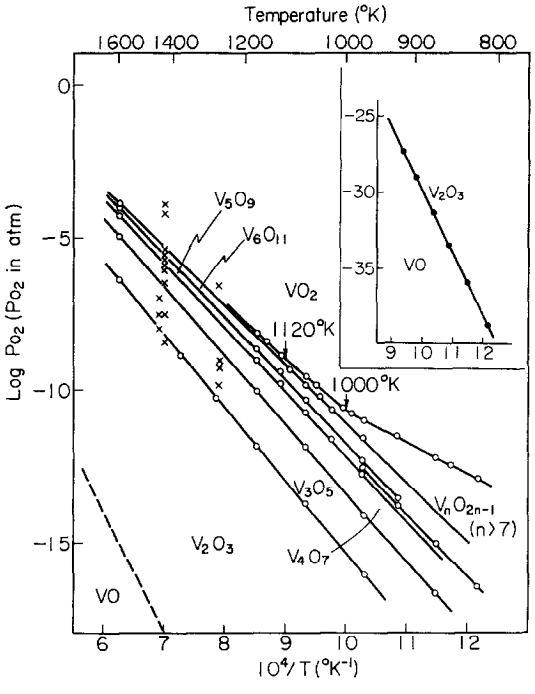

FIG. 2. Equilibrium oxygen pressure vs temperature relation in the V_nO_{2n-1} system: (○) by the solid electrolyte method (×) the quenching method in controlled oxygen atmosphere.

V_5O_9, V_6O_{11} and V_7O_{13}, were confirmed almost in agreement with Andersson's result (*2*). A later electron-diffraction study (*15*) (next section) confirmed, in addition, V_8O_{15} and V_9O_{17} phases.

The preparation of single crystals needed detailed information on the oxygen pressure vs temperature relation of the system. The equilibrium oxygen pressure of the system was measured in the temperature range from 800 to 1300°K by means of a solid state electrolyte cell such as, Pt/adjacent diphasic mixture (V_nO_{2n-1} + $V_{n+1}O_{2(n+1)-1}$)$(ZrO)_{0.85}(CaO)_{0.15}$/air reference electrode/Pt. (*13*, *14*). The result is presented in Fig. 2. The broken line in Fig. 2, which shows the oxygen pressure for the V_2O_3–VO equilibrium, was obtained by an extrapolation of the data indicated in the inset. The equilibrium pressure lines do not cross each other, at least up to 1600°K, indicating that all the phases are stable up to this temperature. Corresponding to the narrow stable field of each compound, the homogeneity range seems to be extremely narrow for these compounds. For phases with $n > 7$, this experiment could not resolve the phase relations.

Structural Study by Electron Diffraction and Microscopy (*15*)

The crystal structure of V_nO_{2n-1} have not previously been so fully studied, owing to the difficulty of the growth of single crystals.[1] Andersson et al., from the structure determination of Ti_5O_9, suggested that the present homologous series is isostructural with the Ti_nO_{2n-1} series and belongs to the same "shear structure" based on the rutile lattice. For Ti_nO_{2n-1}, Bursill et al. (*17*) have confirmed the "shear structure" by electron-diffraction techniques. In Fig. 3, electron-diffraction patterns of V_5O_9 and V_7O_{13} are presented as examples. It can be seen that a unit vector between adjacent main spots—for instance, the vector between (000) and (211)—is divided into n parts by $(n-1)$ extra spots, which suggests a superstructure. In all diffraction patterns, the spots due to the superstructure are found along {211} rutile of the reciprocal lattice. This shows definitely that the present homologous series has the {211} crystallographic shear. These findings agree with the suggestion of Andersson and Jahnberg (*3*). In addition, from these studies it

[1] X-ray crystallographic studies were recently made by Horiuchi et al. (*16*) on single crystals. The results were in essential agreement with those of the present studies and of Andersson and Jahnberg (*3*).

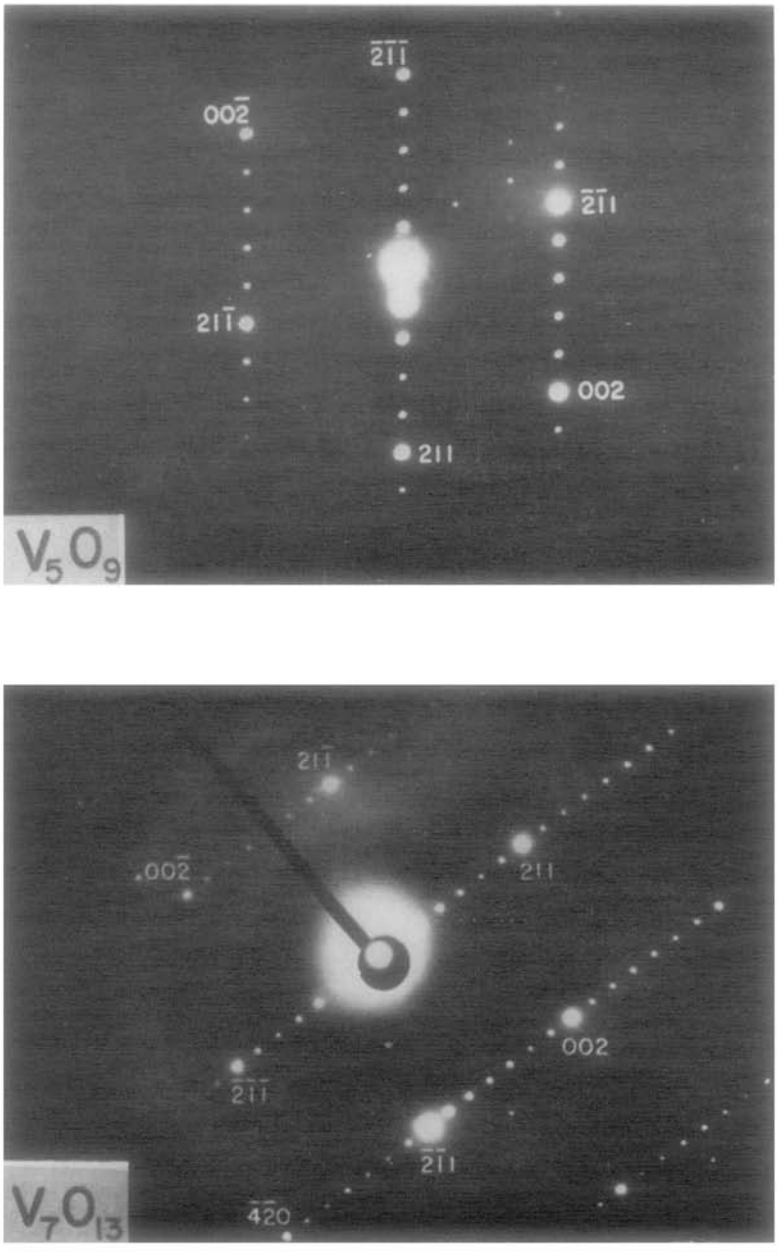

FIG. 3. Electron diffraction patterns of V_5O_9 and V_7O_{13} showing 4 and 6 spots along $g\langle 211\rangle$, respectively.

has been found that the phase from $n = 3$ to $n = 9$ exist as single phases in V_nO_{2n-1}, and that any phase with $n > 9$ does not appear. Bursill et al. (*17*) found that n exists up to 30 or more in the Ti_nO_{2n-1} series, and that there are two kinds of "crystallographic shears"; (121) for $n = 4$–9 and (132) for $n > 9$.

Figure 4 shows the lattice image of V_9O_{17}. The separation between two adjacent shear planes is about 15 Å. Notice that shear planes are arranged with a fairly regular spacing throughout the sample.

Preparation of Single Crystals (*18–20*)

The growth of single crystals was indispensable for studies of various transport phenomena and the refinement of crystal structure. After trial

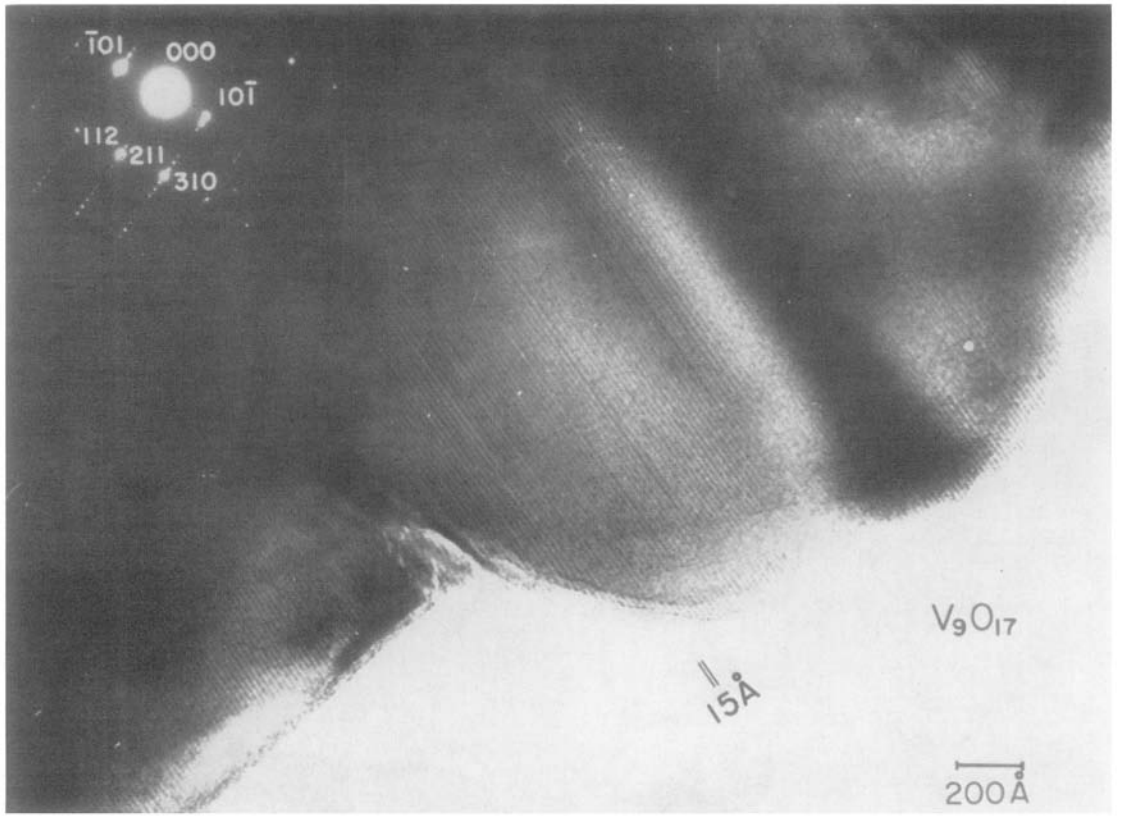

FIG. 4. Lattice image of V_9O_{17}

and error efforts, Nagasawa (*18*), Nagasawa, Bando, and Takada (*19*), and Bando et al. (*20*) found an effective method involving a chemical transport reaction in which $TeCl_4$ was used as a transporting agent. The powder raw material of V_nO_{2n-1} was sealed at one end of an evacuated silica tube together with a few 10 mg of the transporting agent. The end containing the raw material was heated at 1050°C and the other end of the crystallizing zone was at the lower temperature of 1000°C. The following reaction produced fairly large single crystals:

$$V_nO_{2n-1} + TeCl_4 \rightleftharpoons VCl_3 + VCl_4 + TeO_2.$$

Because the equilibrium constant of the above reaction changes sensitively with temperature, at the higher temperature the raw material is transported in the form of VCl_3 and VCl_4 gases and precipitates out as V_nO_{2n-1} single crystals in the crystallizing zone at the lower temperature. A photograph of several crystals thus obtained is presented in Fig. 5. Contamination of the crystals by the carrier gas was unexpectedly small. The impurity of Te was less than 100 ppm (*18*). The compositional inhomogeneity was also tested by electron diffraction and microscopy for 50 or more pieces of finely crushed samples.

These crystals showed excellent homogeneity. Figures 3 and 4 are such examples; no appreciable streaks are found in the diffraction patterns and there is no appreciable inhomogeneity in the spacing of shear planes, as already mentioned.

Electrical Properties (*21–22*)

An earlier study (*23*) of electrical properties made on sintered specimens suggested the presence of phase transitions in the system. The data, however, were not so adequate, because electrical-resistivity measurements were made on polycrystalline samples.

The single crystals described above were large enough to permit the measurement of dc electrical resistivity ρ and thermoelectric power α by ordinary methods. A usual four-point method was applied for the resistivity measurement, and copper was used for the standard of the thermo-

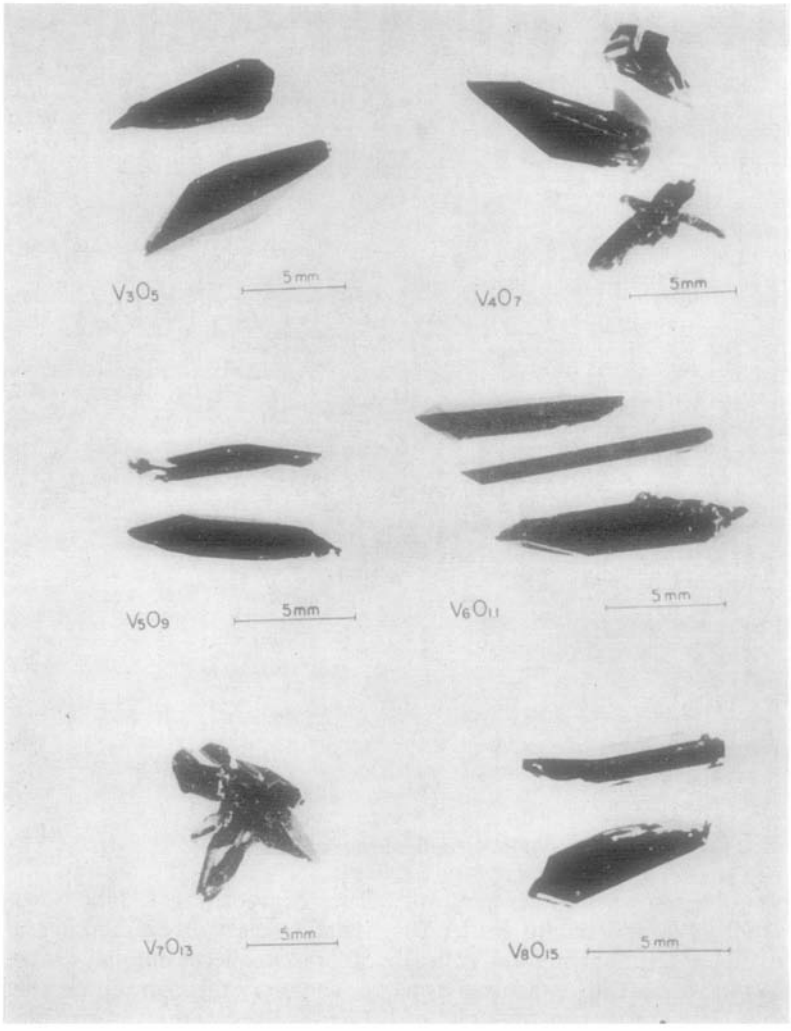

FIG. 5. Single crystals of V_nO_{2n-1}.

electric-power measurement. Typical ρ and α data are shown in Figs. 6 and 7.

All the compositions, except V_3O_5 and V_7O_{13}, have a phase transition at a T_t, from a high-temperature metal to a low-temperature insulator, with a resistivity change of order 10^3–10^7 and with a temperature hysteresis at T_t. During cooling and heating through T_t, breaking of the crystals frequently took place due to crystalline distortion. This suggests that the transition is first-order and has an accompanying crystallographic change.

In the insulating phases, immediately below T_t the activation energies of the conduction are in the order of 0.1 eV, as shown in Table I. The resistivity of the insulating phase increases with decreasing temperature and is saturated at a certain value at low temperatures. The activation energy gradually decreases with decreasing temperature, as is clearly seen in Fig. 6 for V_3O_5, V_4O_7 and V_8O_{15}. This shows that there are many impurity levels in the insulating phases.

The values of the thermoelectric powers are in the range from -10– -20 μV/°K above T_t, which is a characteristic property of metallic conduction. Below T_t the α vs temperature curves are complicated and differ from sample to sample depending on the amount of impurity and non-stoichiometry. The negative values of α below and above T_t, however, indicate that electrons are the main carrier of the conduction both above and below T_t. It is interesting that the V_7O_{13} phase exhibits no transition down to liquid helium temperature.

Magnetic Properties (*11, 12, 24, 25*)

In order to elucidate the mechanism of the metal–insulator transitions in these oxides, the characterization of magnetic properties in both metallic and insulating phases is very important. The magnetic properties, including those of V_2O_3 and VO_2, were studied in detail in the temperature range from 850°K through T_t to liquid helium temperature by the ordinary susceptibility measurement and by Mössbauer spectra.

Figure 8 shows the magnetic susceptibility χ vs temperature curves of the several V_2O_{2n-1} phases around the transition temperatures (*11, 12*). All the phases except V_7O_{13} exhibit a break in the curves. Where there is a metal–insulator transition, an abrupt break occurs at the temperature T_t. These breaks have a shape apparently similar to that of an antiferromagnet. However, the abrupt breaks at T_t are not due to paramagnetic–antiferromagnetic transitions, as is shown by Mössbauer experiments. The susceptibility curves above T_t nearly obey a Curie–Weiss law $\chi = [C/(T-\theta)] + \chi_0 + \chi_{diam}$, where χ_0 is the temperature-independent paramagnetism, χ_{diam} the ion-core and orbital diamagnetism, C the Curie–Weiss constant and θ the paramagnetic Curie temperature. The Curie–Weiss constant C_{obs}, the effective localized moment μ_{eff} and the state density $D(\xi)$ assuming Pauli paramagnetism for χ_0 were calculated and are listed in Table II. The Curie–Weiss constants C_{obs} and the μ_{eff} values are very close to those (C_{calc} and μ_{calc}) calculated on the assumption that all the tetravalent and trivalent vanadium ions are in a localized paramagnetic state. It is also to be noticed that an extremely large electronic state density is expected for V_4O_7, V_5O_9, V_6O_{11} and V_7O_{13} phases, as discussed below.

For the study of magnetic properties, the Mössbauer experiment is simple and useful. Shinjo and Kosuge (*26*) found an antiferromagnetism in V_2O_3 by the Mössbauer spectra on

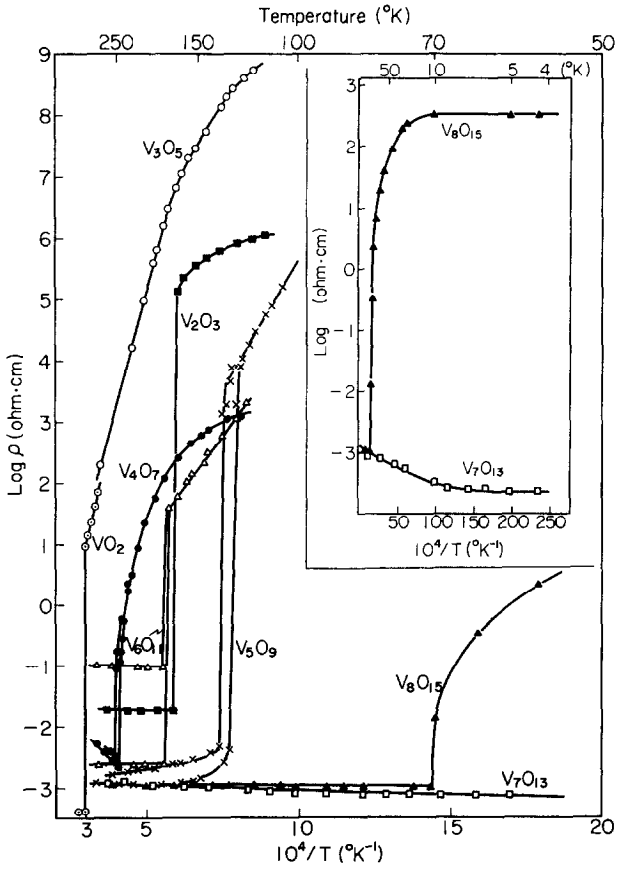

FIG. 6. Electrical resistivity ρ vs reciprocal temperature curves.

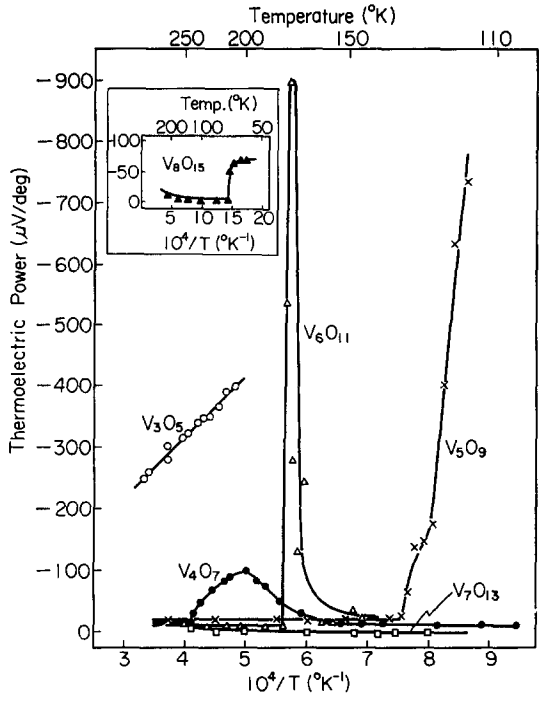

FIG. 7. Thermoelectric power α vs reciprocal temperature curves.

an ^{57}Fe-doped sample, which later was confirmed by NMR (*27*) and spin-flipping neutron diffraction (*28*).

Figure 9 shows the spectrum of ^{57}Fe doped V_2O_3 below and above T_t (*26*). The hyperfine splitting, which verifies the antiferromagnetism, disappears abruptly at T_t. On the other hand, VO_2 was confirmed to be paramagnetic above and also below T_t (*29*). To investigate the properties of the V_nO_{2n-1} series around their transition temperatures, powder samples of V_4O_7 and V_5O_9, both doped with 1% ^{57}Fe, were prepared. Figure 10 shows the absorption spectra for V_4O_7 above and below T_t. A similar result was also obtained for V_5O_9. The absence of hyperfine splitting below T_t for both cases suggests that these phases are paramagnetic in the insulating state immediately below the transition point.

These results, including those of V_2O_3 and VO_2, indicate that the antiferromagnetic ordering is not a necessary condition for the metal–insulator transition; the conclusion is in agreement with the discussions of Goodenough (*8*) and Adler (*6*). However, there is need to study the magnetic properties from the transition temperature down to liquid helium temperature to get more information on the insulating state.

Figure 11 shows the susceptibility data in this temperature range. For each compound there appears another anomalous peak at a lower temperature T_A, suggesting antiferromagnetic ordering. Also the susceptibility nearly obeys a

TABLE I

ELECTRICAL PROPERTEIS OF V_nO_{2n-1}

V_nO_{2n-1}	Characteristic of electrical conduction	T_t (°K) cooling	T_t (°K) heating	Electrical resistivity of metallic phase (Ω cm)	Thermoelectric power of metallic phase (μV/deg)	Activation energy of insulating (semiconducting) phase (eV)	Fermi energy (eV)
V_3O_5	Insulator (semiconductive, *n*-type)	—	—	—	—	0.4	0.1
V_4O_7	Metal-to-insulator (semiconductive, *n*-type)	244	250	10^{-2}–10^{-3}	−10	0.08–0.1	0.15
V_5O_9	Metal-to-insulator (semiconductive, *n*-type)	129	135	10^{-2}–10^{-3}	−20	0.1–0.2	0.2
V_6O_{11}	Metal-to-insulator (semiconductive *n*-type)	174	177	10^{-2}–10^{-3}	−10	0.12	—
V_7O_{13}	Metal	—	—	10^{-3}	0–−1	—	—
V_8O_{15}	Metal-to-insulator (semiconductive, *n*-type)	—	70	10^{-3}	−5–−20	0.13	—

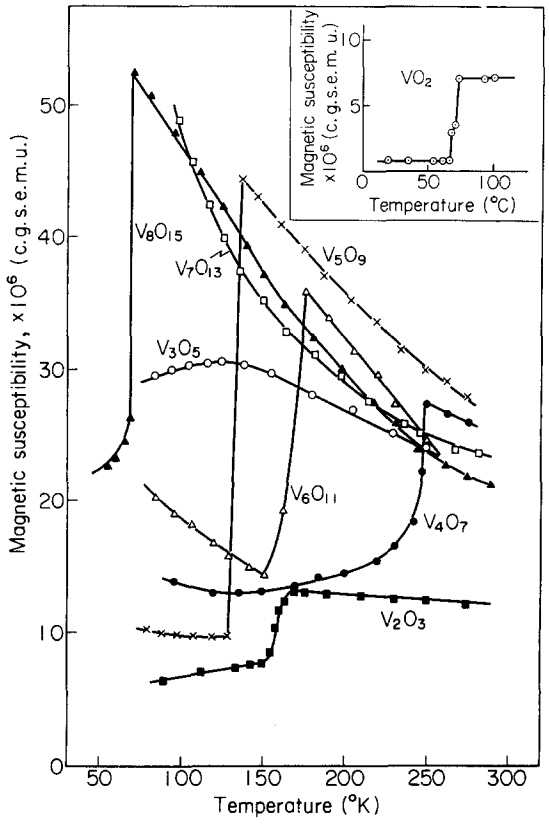

FIG. 8. Temperature dependence of the magnetic susceptibility.

Curie–Weiss law in the temperature range $T_A < T < T_t$, where the susceptibility is sharply reduced compared with that of the region $T > T_t$. The data are listed in Table II.

The relations between T_A and T_t are classified into the following three types;

i. $T_A < T_t$: V_4O_7, V_5O_9, V_6O_{11}, V_8O_{15}

ii. No T_t (metallic down to liquid helium temperature) with T_A: V_7O_{13}

iii. No T_t (semiconductive down to liquid helium temperature) with a broad-peak T_A: V_3O_5.

In order to elucidate the origin of these anomalies at T_A, the Mössbauer spectra of ^{57}Fe-doped V_3O_5, V_4O_7 and V_7O_{13} were studied, each of which was selected as a representative of the above groups (*24*). The preparation method of the doped samples was similar to that of previous experiments.

The results are shown in Fig. 12. All the samples are antiferromagnetic at 4.2°K. The internal fields in V_3O_5, V_4O_7 and V_7O_{13} at 4.2°K are about 390, 400 and 440 kOe, respectively. The field, in the cases V_4O_7 and V_7O_{13}, decreases and vanishes near T_A, obeying a Brillouin function, so the temperature T_A seems to correspond to a Neel temperature T_N. It is interesting, however, to note that the internal field of V_3O_5 disappears at about 69°K, quite a bit lower than the temperature of the broad peak in the χ–T curve. The

TABLE II

MAGNETIC PROPERTIES OF V_nO_{2n-1}

Phase	T_t[a] (°K)	T_N[b] (°K)	$T > T_t$ C_{obs}	C_{cal}[c]	μ_{eff} (μ_B)	θ	$\chi_0 \times 10^4$ (e.m.u. mole^{-1})	$D_{(\xi)}$[d]	$T_t > T > T_N$ C_{obs}	μ_{eff} (μ_B)
V_2O_3	168	168	0.82	0.98	2.96	−600	320	9.8	—	—
V_3O_5	—	70	0.78	0.77	2.51	−97	85	—	—	—
V_4O_7	250	40	0.57	0.67	2.14	−21	275	8.6	0.057	0.699
V_5O_9	135	30	0.57	0.61	2.13	−18	290	9.0	0.056	0.674
V_6O_{11}	170	23	0.53	0.58	2.06	−33	287	8.8	0.24	1.364
V_7O_{13}	—	43	0.52	0.55	2.04	−38	162	5.0	—	—
V_8O_{15}	70	7	—	—	—	—	—	—	—	—
VO_2	340	—	0.68	0.37	2.33	−629	61	1.9	—	—

[a] Transition temperature.

[b] Neel temperature.

[c] C_{cal} is the Curie constant calculated assuming the localized V^{3+} and V^{4+} ions.

[d] State density of electron (electrons per eV per V_{atom}) at Fermi level ξ; calculated assuming Pauli paramagnetism for χ_0.

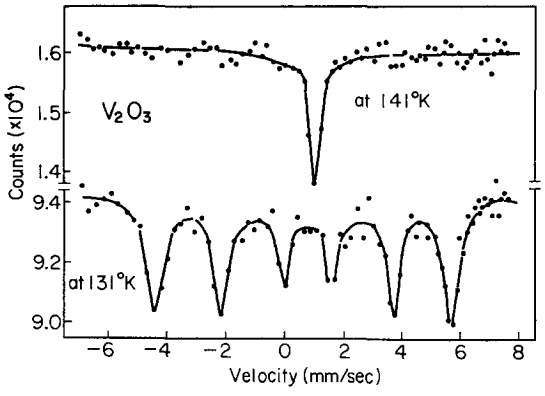

FIG. 9. Mössbauer absorption spectra of ^{57}Fe-doped V_2O_3 above and below T_t (=140°K).

metallic conduction of V_7O_{13} with antiferromagnetic ordering is also interesting—this may be the first example of an antiferromagnetic oxide with metallic character.

Kosuge (*11*) accounted for the reduction of the magnetic susceptibility in the insulating state below T_t by the cooperative pairing of both the V^{3+}–V^{3+} and V^{4+}–V^{4+} ions; applying Goodenough's model for VO_2. However, to account for the above results and the presence of a magnetic moment in the temperature range between T_t and T_N (Table II), one must at least assume that the V^{3+}–V^{3+} pairing is incomplete and that the remaining moments undergo long-range antiferromagnetic order below T_N.

Heat and Entropy of Transition

Thermodynamic information concerning the transition is very important. The heat of transition ΔH in the V_nO_{2n-1} phases, including V_2O_3 and VO_2, was measured by a scanning calorimeter of Rigakudenki. The error of the measurement was about 5%

The data are listed in Table III with the data of entropy change $\Delta S = \Delta H/T_t$. The data for V_2O_3 and VO_2 are in good agreements with those of Feinleib and Paul (*30*) and Cook (*31*). The entropy change increases with increasing n.

Low-Temperature Specific Heat

Measurement of the low-temperature specific heat gives important information on the electronic state. The susceptibility measurements described above suggested a large state density for the V_nO_{2n-1} metallic phases (Table II). McWhan et al. (*32*) measured low-temperature specific heats of V_4O_7, V_7O_{13} and $V_2O_{3.04}$ among which V_7O_{13} and $V_2O_{3.04}$ (*33–35*) are metallic down to liquid helium temperature. The measurement was made by the pulsed method of Morin and Maita (*36*). The results are shown in Fig. 13.

An extremely large linear term γ was obtained for the metallic phases V_7O_{13} ($\gamma = 80 \times 10^{-4}$ cal/°K^2 mole) and $V_2O_{3.04}$ ($\gamma = 130 \times 10^{-4}$ cal/°K^2 mole). The electronic state density of V_7O_{13} calculated from this γ is 7, in good agreement with that ($D(\xi) = 5.00$) calculated from χ_0 (see Table II)—to the extent that it sounds somewhat "by chance." These γ values are much larger than those of normal metals, for which typically $\gamma = 5 \times 10^{-4}$ cal/°K^2.

McWhan et al. (*37*) previously found a large $\gamma(90 \times 10^{-4}$ cal/°K^2 mole) for metallic $(V_{0.92}Ti_{0.08})_2O_3$. These results suggest that the electronic density of states is greatly enhanced in transition metal oxides that are near metal–insulator transitions.

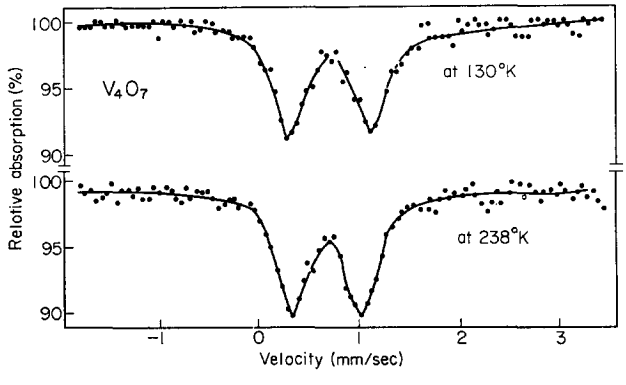

FIG. 10. Mössbauer absorption spectra of ^{57}Fe-doped V_4O_7 above and below T_t (=235°K).

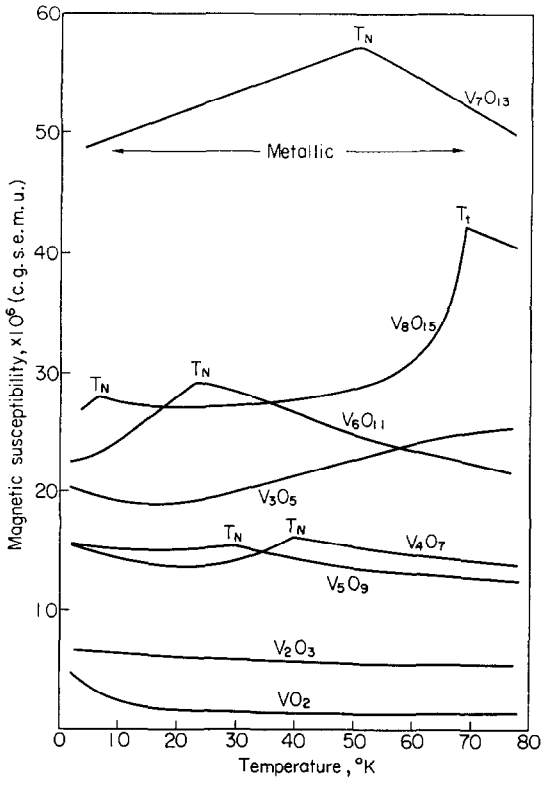

FIG. 11. Magnetic susceptibility curves for V_nO_{2n-1} below T_t.

The magnetic-ordering contributions to the heat capacity of V_4O_7 and V_7O_{13} can be easily estimated by a simple substraction, if one assumes that the lattice contributions for both cases are similar to that of VO_2 scaled to the same number of atoms, and that the linear term for V_7O_{13} is constant up above magnetic transition point at

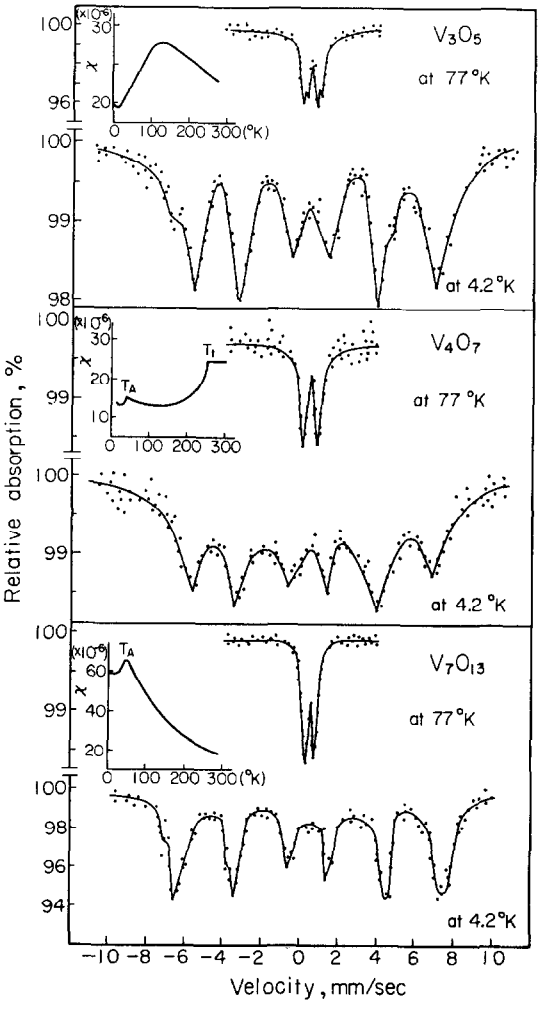

FIG. 12. Mössbauer absorption spectra for V_3O_5, V_4O_7 and V_7O_{13} at lower temperature.

TABLE III

HEAT AND ENTROPY CHANGE OF TRANSITION

V_nO_{2n-1}	Molecular formula	Heat of transition (cal/mole); ΔH	Transition temp. T_t (°K)	Entropy change of transition ΔS (cal/mole deg); $(\Delta H/T_t)$
V_2O_3	$VO_{1.50}$	207	168	1.22
V_3O_5	$VO_{1.66}$	—	—	—
V_4O_7	$VO_{1.75}$	142	250	0.57
V_5O_9	$VO_{1.80}$	215	135	1.59
V_6O_{11}	$VO_{1.833}$	222	170	1.31
V_7O_{13}	$VO_{1.857}$	—	—	—
VO_2	VO_2	1012	340	3.0

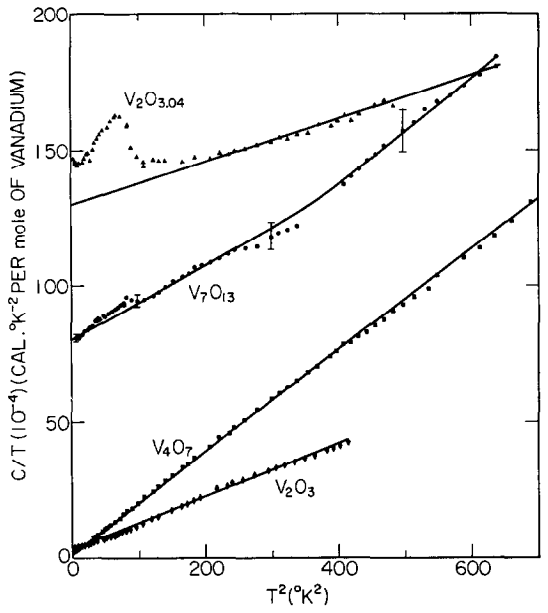

FIG. 13. Specific heat of V_4O_7, V_7O_{13}, $V_2O_{3.04}$ and V_2O_3 plotted as C/T vs T^2 to show the large linear term in the metallic phases. The errors in the data for V_4O_7 and $V_2O_{3.04}$ are 1% but the error for V_7O_{13} is indicated by the bars [McWhan et al. (*32*)].

43°K. The calculated magnetic entropies up to 53°K are 0.32 ± 0.01 cal°K^{-1} per $VO_{7/4}$ and 0.31 ± 0.1 cal°K^{-1} per $VO_{13/7}$, respectively, for V_4O_7 and V_7O_{13} (*32*). Both of these numbers are far below the values calculated for the ordering of localized V^{3+} and V^{4+} ions (1.8 and 1.6 for V_4O_7 and V_7O_{13}, respectively). Even if the V^{4+} ions in V_4O_7 form pairs to produce nonmagnetic states, the V^{3+} ions would contribute 1/2R ln 3–1.1 cal°K^{-1} $VO_{7/4}$ (V_4O_7 contains equal amounts of V^{3+} and V^{4+} ions, which accounts for the factor 1/2. So, if the pairing model is adopted, one must assume that either most of the V^{3+} ions also pair to form nonmagnetic states, or that pairing of the V^{3+} ions reduces the net moment on each V^{3+} ion. One can also consider that a substantial amount of short-range magnetic order persists to well above the magnetic-ordering temperature in insulating V_4O_7.

McWhan et al. (*37*) suggested that both the enhanced electronic density of states reflected in the large linear term and the small magnetic entropy below the ordering temperature in V_2O_3 are evidence for a highly correlated electronic system. From this point of view, the transition in the present V_nO_{2n-1} system is similar to the case of V_2O_3, and may include the many body effect.

Discussion

The present studies on the V_nO_{2n-1} series confirm that the phases with $n = 4, 5, 6$ and 8 have temperature-induced metal–insulator transitions and that all the phases with $n = 3, 4, 5, 6, 7, 8$ order magnetically. Whereas magnetic order occurs in the insulating state ($T_N < T_t$) if $n = 4, 5, 6$ or 8, V_7O_{13} was found to have metallic behavior down to 4.2°K. These properties are summarized in the phase diagram of Fig. 14. The magnetic-ordering temperatures of the insulating phases change smoothly with n, whereas the metal–insulator transition temperatures change quite irregularly. The behavior of V_2O_3 is unique. It exhibits a typical metal–insulator transition, but the insulating phase is antiferromagnetic for all $T < T_t$. These properties of the V_nO_{2n-1} series appear difficult to account for by a single theoretical model.

Several theoretical models have been proposed for the transitions in V_2O_3 and VO_2. Goodenough (*38*) first suggested that the transition is associated with the formation of V–V homopolar

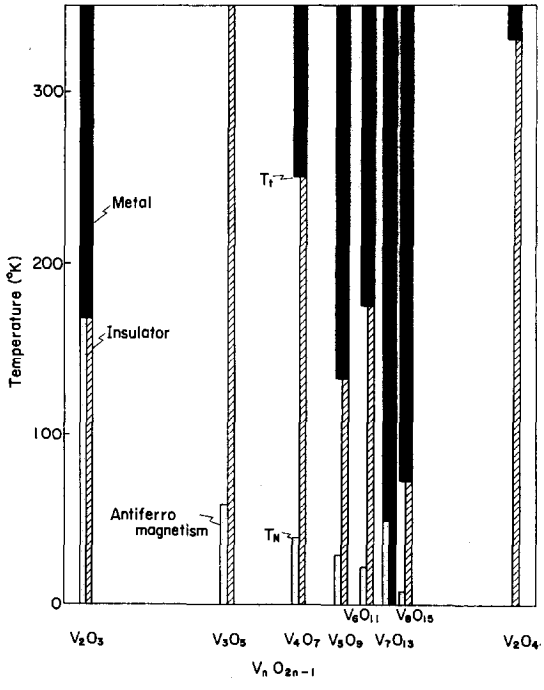

FIG. 14. Magnetic and electrical phase diagram for V_nO_{2n-1}. ■ metal; ■ insulator; ▨ antiferromagnetic.

bonds (pairing model). He subsequently generalized this model to any mechanism that would change the periodicity of the translational symmetry (*39*), and Adler (*6*), Adler and Brooks (*40*), and Adler et al. (*41*) simultaneously developed a similar, but more formal, model in which they explicitly neglected the influence of electron correlations and attribute the origin of the transition in V_2O_3 and VO_2 to crystalline distortions (crystalline distortion theory). The above two models consistently suggested the importance of electron–lattice interactions and showed that the magnetic ordering is not a necessary condition. On the other hand, Mott and Zinamon (*7*) and Mott (*42*, *43*) have emphasized the importance of electron correlations for the transition. According to his theory, the energy gap in the insulating state originates from the electron-correlation effect—Mott–Hubbard gap —and the ground state of the insulating phase may be antiferromagnetic. A recent paper by McWhan and Remeika (*45*) suggested that the transitions in chromium or titanium doped V_2O_3 are Mott-type transitions. Goodenough (*8*) has emphasized more recently that more than one mechanism is operative in the transitions found in V_2O_3 and VO_2.

Each of these models includes plausible ideas for understanding the V_nO_{2n-1} system. However, the nonintegral number of *d*-electrons per cation in the V_nO_{2n-1} phases makes it difficult to apply Mott's explanation to the transitions in these materials—at least in its simplest form. Nevertheless, the magnetic ordering exhibited in these materials at lower temperature is in an accordance with this theory.

Although it is not possible to criticize the crystalline distortion theory until the crystallographic data on the insulating phases are obtained, the theory would seem to have difficulty in explaining univocally all the transitions, including the metallic V_7O_{13} phase, without ad hoc assumptions.

Kosuge (*11*), as mentioned above, showed that the reduction of the magnetic susceptibility in the insulating phase could be well explained by the *d*-electron pairing model proposed by Goodenough, but one must assume an incomplete pairing to explain the presence of a small magnetic moment (Table II) and a small magnetic entropy of the insulating state. Furthermore, the metallic properties of these materials above the transition temperature are difficult to understand when one considers that the magnetic susceptibility follows a Curie–Weiss law based on localized V^{3+} and V^{4+} ions. For instance, for V_7O_{13} the Curie constant C_{obs} is 0.52 (calculated value ~0.55) and the Weiss temperature θ is −38°K while the observed ordering temperature is 43°K. This fact suggests that the band is narrow and strongly correlated. However, the large γ value of V_7O_{13} ($\gamma = 80 \times 10^{-4}$ cal °K^{-2}/V atom) indicates that the material is truly metallic. Brinkman and Rice (*46*) have suggested that such a large γ together with a small magnetic entropy are evidence for a highly correlated electronic system in which electrons are itinerant, but have a strong interaction with each other. In their theory, the assumption was made that the electron–lattice interaction is weak.

However, if the large γ originates from a strong correlation effect of the electrons, as McWhan et al. suggest (*37*), then there might be a complicated behavior in the temperature dependence of γ. Therefore we need much information about the lattice entropy, that is, the change of the phonon spectrum at the transition.

Concluding Remarks

We have found that the phases V_nO_{2n-1} lying between V_2O_3 and VO_2 have temperature-induced metal–insulator transitions. Their structural, thermodynamic, magnetic and electrical properties have been studied on powder or single crystals. A notable result is the observation of magnetic ordering at a lower temperature than the metal–insulator transition. In addition, V_7O_{13}, which remains metallic down to 4.2°K, is a metallic antiferromagnet below 43°K. It was pointed out that existing theories, in their simplest form, apparently do not provide a satisfactory explanation of the metal–insulator transitions.

An extremely large linear term of the electronic specific heat of V_7O_{13} was found, suggesting that the transition in this series is mainly electronic in origin. The striking change of electrical properties brought about by relatively small structural or compositional alterations in this series of materials suggest that highly detailed theoretical treatments will be needed for a satisfactory degree of understanding.

References

1. E. Hoschek and W. Klemm, *Z. Anorg. Chem.* **242**, 63 (1939).
2. G. Andersson, *Acta Chem. Scand.* **8**, 413 (1963).

3. S. ANDERSSON AND L. JAHNBERG, *Ark. Kemi* **21**, 413 (1963).
4. A. D. WADSLEY, *in* "Non-stoichiometric Compounds" (L. Mandelcorn, Ed.). Academic Press, New York (1964).
5. F. J. MORIN, *Phys. Rev. Lett.* **3**, 34 (1959).
6. D. ADLER, *in* "Solid State Physics" (H. Ehrenreich, F. Seitz, and D. Turnbull, Eds.), Vol. 21, p. 1. Academic Press, New York (1968); *Rev. Mod. Phys.* **40**, 714 (1968).
7. N. F. MOTT AND Z. ZINAMON, Report. Prog. Phys. **33**, 881 (1970).
8. J. B. GOODENOUGH, "Progress in Solid State Chemistry" (Howard Reiss, Ed.), Vol. 5, pp. 145–399. Pergamon, Elmsford, New York (1971).
9. G. J. HYLAND, *J. Solid State Chem.* **2**, 318 (1970).
10. J. P. SUCHET, "Crystal Chemistry and Semiconductor." Academic Press, New York (1971).
11. K. KOSUGE, *J. Phys. Chem. Solid* **28**, 1613 (1964).
12. T. TODA, K. KOSUGE, AND S. KACHI, *Nippon Kagaku Zasshi* **87**, 1311 (1961).
13. H. OKINAKA, K. KOSUGE AND S. KACHI, *Jap. J. Appl. Phys.* **9**, 224 (1970).
14. H. OKINAKA, K. KOSUGE, AND S. KACHI, *Trans. Jap. Inst.* **12**, 44 (1971).
15. K. KOSUGE, H. OKINAKA, S. KACHI, K. NAGASAWA, Y. BANDO, AND T. TAKADA, *Jap. J. Appl. Phys.* **9**, 1004 (1970).
16. H. HORIUCHI, M. TOKONAMI, N. MORIMOTO, K. NAGASAWA, Y. BANDO, AND T. TAKADA, *Mater. Res. Bull.* **6**, 833 (1971).
17. L. A. BURSILL, B. G. HYDE, O. TERASAKI, AND D. WATANABE, *Phil. Mag.* **20**, 347 (1969).
18. K. NAGASAWA, *Mater. Res. Bull.* **6**, 853 (1971).
19. K. Nagasawa, Y. BANDO, AND T. TAKADA, *Jap. J. Appl. Phys.* **8**, 1262, 1267 (1969); **9**, 407 (1970).
20. Y. BANDO, K. NAGASAWA, Y. KATO, AND T. TAKADA, *Jap. J. Appl. Phys.* **8**, 633 (1969).
21. H. OKINAKA, K. NAGASAWA, K. KOSUGE, Y. BANDO, T. TAKADA, AND S. KACHI, *J. Phys. Soc. Jap.* **27**, 1366 (1969); **28**, 798, 803 (1970); **29**, 245 (1970).
22. H. OKINAKA, K. NAGASAWA, K. KOSUGE, Y. BANDO, T. TAKADA, AND S. KACHI, *Phys. Lett.* **33A**, 370 (1970).
23. S. KACHI, T. TAKADA, AND K. KOSUGE, *J. Phys. Soc. Jap.* **18**, 1839 (1963).
24. H. OKINAKA, K. KOSUGE, S. KACHI, M. TAKANO, AND T. TAKADA, *J. Phys. Soc. Jap.*, **32**, 1148 (1972).
25. H. OKINAKA, thesis of Kyoto Univ. Faculty of Science (1972).
26. T. SHINJO AND K. KOSUGE, *J. Phys. Soc. Jap.* **21**, 2622 (1966).
27. J. UMEDA, H. KUSUMOTO, K. NARITA, AND E. YAMADA, *J. Chem. Phys.* **42**, 1458 (1965).
28. R. M. MOON, *J. Appl. Phys.* **41**, 883 (1970).
29. K. KOSUGE, *J. Phys. Soc. Jap.* **22**, 551 (1969).
30. J. FEINLEIB AND W. PAUL, *Phys. Rev.* **155**, 841 (1967).
31. O. A. COOK, *J. Amer. Chem. Soc.* **69**, 331 (1947).
32. D. B. MCWHAN, J. P. REMEIKA, J. P. MAITA, H. OKINAKA, K. KOSUGE, AND S. KACHI, *Phys. Rev.* in press.
33. M. NAKAHIRA, S. HORIUCHI, AND H. OOSHIMA, *J. Appl. Phys.* **41**, 836 (1970).
34. V. N. NOVIKOV, B. A. TALLERCHIK, E. I. GINDIN, AND V. G. PROKHVATILOV, *Sov. Phys. Solid State* **12**, 2061 (1971).
35. D. B. MCWHAN, A. MENTH, AND J. P. REMEIKA, *J. Phys. (Paris)* **32**, C1-1079 (1971).
36. F. J. MORIN AND J. P. MAITA, *Phys. Rev.* **129**, 1115 (1963).
37. D. B. MCWHAN, J. P. REMEIKA, T. M. RICE, W. F. BRINKMAN, J. P. MAITA, AND A. MENTH, *Phys. Rev. Lett.* **27**, 941 (1971).
38. J. B. GOODENOUGH, *Phys. Rev.* **137**, A987 (1965), *Bull. Soc. Chim. Fr.* p. 1200 (1965).
39. J. B. GOODENOUGH, *Czech. J. Phys.* **B17**, 304 (1967).
40. D. ADLER AND H. BROOKS, *Phys. Rev.* **152**, 826 (1967).
41. D. ADLER, J. FEINLEIB, H. BROOKS, AND W. PAUL, *Phys. Rev.* **152**, 851 (1967).
42. N. F. MOTT, *Phil. Mag.* **6**, 287 (1961).
43. N. F. MOTT, *Rev. Mod. Phys.* **40**, 677 (1968).
44. N. F. MOTT, *Phil. Mag.* **24**, 1 (1971).
45. D. B. MCWHAN AND J. P. REMEIKA, *Phys. Rev. B* **2**, 3734 (1970).
46. W. F. BRINKMAN AND T. M. RICE, *Phys. Rev. B* **2**, 4302 (1970).